Spatial dichotomy of quasiparticle dynamics in underdoped thin-film $YBa_2Cu_3O_{7-\delta}$ superconductors

C. W. Luo,[1] C. C. Hsieh,[1] Y.-J. Chen,[1] P. T. Shih,[1] M. H. Chen,[1] K. H. Wu,[1] J. Y. Juang,[1,3] J.-Y. Lin,[2] T. M. Uen,[1] and Y. S. Gou[3]

[1]*Department of Electrophysics, National Chiao Tung University, Hsinchu, Taiwan, Republic of China*

[2]*Institute of Physics, National Chiao Tung University, Hsinchu, Taiwan, Republic of China*

[3]*Department of Physics, National Taiwan Normal University, Taipei, Taiwan, Republic of China*

(Received 18 September 2006; revised manuscript received 28 April 2006; published 22 November 2006)

By the spatial-temporal-resolved femtosecond spectroscopy on well-textured (110)- and (100)-YBCO thin films, two distinctly temperature-dependent characteristics of quasiparticle relaxation in the nodal and antinodal directions are clearly identified. One temperature dependence associated with a high-energy gap has been observed along the *ab* diagonal for the whole hole-doping region and along the *b* axis except near optimal doping, while the other temperature dependence related to the opening of the superconducting gap appears along *b* axis regardless of the hole concentration. This spatial dichotomy between the nodal and antinodal quasiparticle dynamics and the evolution of gap symmetry with hole doping are discussed for enlightenment on the nature of the phase diagram of hole-doped cuprates. These strongly suggest that the two characteristics may have different physical origins and compete with each other.

DOI: 10.1103/PhysRevB.74.184525 PACS number(s): 74.25.Gz, 74.78.Bz, 74.81.Bd, 78.47.+p

I. INTRODUCTION

Elucidation of the phase diagram of high-T_c superconductivity has been one of the most demanding intellectual challenges. Usually different theoretical models of high-T_c superconductivity propose different phase diagrams.[1,2] Therefore, experimental investigation of the phase diagram is the key to distinguishing the appropriate theory of high-T_c superconductivity, which is considered by many to remain elusive. Very recently, angle-resolved photoemission spectroscopy (ARPES) indicated a dichotomy between nodal and antinodal excitations.[3–5] However, the spatial anisotropy of quasiparticle (QP) relaxation dynamics and how the evolution of the gap symmetry with doping have remained to be revealed. The time-domain spectroscopy,[6–10] which probes the dynamics of the electronic states intimate to superconductivity, has proven to be a powerful tool to provide new insights into the fundamental nature of both the pseudogap and the superconducting gap.[7–10] Suggested by the previous time-resolved spectroscopy experiments,[11–19] the amplitude and picosecond scale relaxation time of the transient reflectivity change ($\Delta R/R$) observed below T_c are directly associated with the opening of the superconducting gap. For example, Kabanov *et al.*[17] have calculated the temperature dependence of the photoexcited QP density and concluded that $\Delta R/R$ is determined by two gaps with different energy scales and temperature dependences. Recently, it has been demonstrated that the polarized time-resolved spectroscopy on well-oriented samples provides prominent information about the symmetry of the superconducting gap[9] and the QP relaxation along various crystalline orientations.[10] Following these ideas, the experiments carried out here, directly reveals the spatial dichotomy between the nodal (*ab* diagonal) and antinodal (*a* or *b* axis) QP relaxation dynamics as well as the respective evolution of the gap symmetry with hole doped YBCO. The analysis does not involve any specific theoretical model and consequently the results are model independent.

II. EXPERIMENTAL SETUP AND RESULTS

The (001)-, (100)-, and (110)-oriented YBCO films used in this study were prepared by pulsed laser deposition. The characterization and manipulation of the oxygen content on the films were discussed in detail elsewhere.[20–23] Briefly, the orientation alignment of each set of films is better than 97%. The orientation- and time-resolved femtosecond spectroscopy was carried out by the pump-probe scheme with 20 fs pulses at a central wavelength of 800 nm, as described in Ref. 9.

Figure 1(a) shows the typical $\Delta R/R$ curves on the *ab* plane of (001) YBCO films with T_c=90.4 K in the normal and superconducting states, respectively. The significant distinction between these two states could be easily interpreted by the following context, which is generally accepted as the protocols in the pump-probe experiments. Namely, the pump pulse excites the electron-hole pairs that relax to the states in the vicinity of the Fermi energy (E_F) by various scattering mechanisms (e.g., electron-electron or electron-phonon scattering). This process occurs in the normal state ($T>T_c$) within a subpicosecond time scale.[17,24] The presence of a gap near E_F leads to the carrier accumulation in the quasiparticle states above the gap in the superconducting state ($T<T_c$). This, in turn, gives rise to a transient change in reflectivity ($\Delta R/R$) to be detected by a second laser (probe) pulse as a function of the time delay (t) between the pump and probe pulses. The amplitude and characteristic relaxation time of the measured $\Delta R/R$ thus give important information of the number of the accumulated QPs and the amplitude of the gap.[9,11,12,17] Since the *ab* plane results from (001) YBCO films are the averaged result of those from the *a* axis, *b* axis, and *ab* diagonal, the spatial resolution of the QP dynamics is largely missing. In order to separate the ultrafast responses along the *b* axis and the *ab* diagonal, we have used (100)- and (110)-YBCO films, respectively, with polarized pump and probe beams for the measurements. The typical results

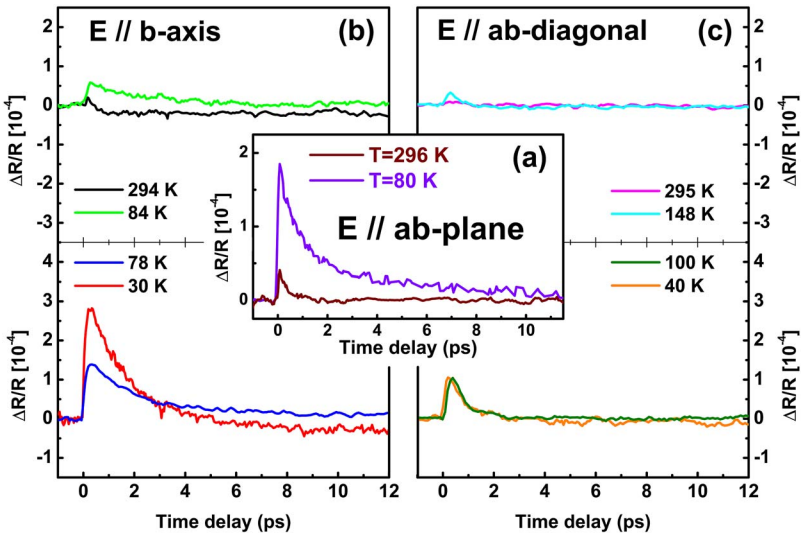

FIG. 1. (Color online) The temperature dependence of $\Delta R/R$ (a) in the *ab* plane measured in a (001) YBCO film with T_c=90.4 K; (b) along the *b* axis measured in a (100) YBCO film with T_c=89.7 K; and (c) along the *ab* diagonal measured in a (110) YBCO film with T_c=90.2 K.

are shown in Figs. 1(b) and 1(c). There are quite significant distinctions, similar to Fig. 1(a), between the normal and the superconducting states (not only in the magnitude, but also in the characteristics of the relaxation) for the $\Delta R/R$ along the *b* axis near optimal doping (T_c=89.7 K). For the *ab* diagonal, however, the magnitude of $\Delta R/R$ starts to change at $T\sim 150$ K (well above T_c=90.2 K) and reaches a constant value below $T\sim 100$ K, and the characteristics of relaxation are almost independent of *T* for the whole temperature range where the transient behavior occurs. Especially, $\Delta R/R$ is quantitatively illustrated in Fig. 2 where the normalized $\Delta R/R$ as a function of the reduced temperature (T/T_c) is shown.

Near optimal doping, the data along the *b* axis [Fig. 2(b)] are dramatically different from those along the *ab* diagonal [Fig. 2(c)]. The anomaly just near T_c, called "*A*-type temperature dependence," is suggestive of the opening of the superconducting gap that is absent along the *ab* diagonal. On the other hand, the amplitude of $\Delta R/R$ measured along the *ab* diagonal is persistent to temperatures well above T_c [Fig. 2(c)] and this behavior, called "*B*-type temperature dependence," may be governed by another order parameter, e.g., high-energy gap. Unlike the two cases just mentioned above, the data of the *ab* plane of (001) YBCO [Fig. 2(a)] cannot be described by either the behavior of *A* or *B* temperature dependence alone. Nonetheless, it can be explained by the combination of both types of the temperature dependence. The present study, thus for the first time, distinguishes two kinds of QP relaxation dynamics in CuO_2 planes of YBCO to display their respective orientation characteristics in real space.

As the YBCO sample becomes further underdoped [T_c =77.9 K and 55.7 K, this was achieved on *one single (100) YBCO film* by the method described in Ref. 23], $\Delta R/R$ appears to have two distinct components along the *b* axis [Fig. 3(a) for T_c=77.9 K, i.e., hole concentration p=0.118].[25] The positive component of $\Delta R/R$ starts to appear at temperature well above T_c ($T\sim 160$ K) and exhibits the *B*-type temperature dependence, which could be associated with the high-energy gap. As $T<T_c$ (e.g., T=75 K), the negative component of $\Delta R/R$ appears and its characteristics are close to the *A*-type temperature dependence which is expected from the opening of the superconducting gap.[27] This indicates that two types of the temperature dependence have been both observed at this underdoping level for $\mathbf{E}//b$ axis. In the same (100) YBCO film with further underdoping (T_c=55.7 K, p =0.091), the similar behavior has also been observed along the *b* axis except that the amplitude of $\Delta R/R$ diminishes more rapidly with increasing temperature, e.g., Fig. 3(b). Furthermore, $\Delta R/R$ along the *ab* diagonal for several underdoped cases [T_c=80.8 K (p=0.123) and 62.2 K (p=0.098)] can be studied through *one single (110) YBCO film*. The normalized $\Delta R/R$ increases gradually with decreasing temperature for all doping levels [Fig. 3(c)]. Along this crystalline orientation, only the *B*-type temperature dependence of $\Delta R/R$ was observed either below or above T_c [cf. Fig. 1(c)].

III. DISCUSSION

In order to quantify the systematic variation in the temperature dependence of the *B*-type temperature dependence

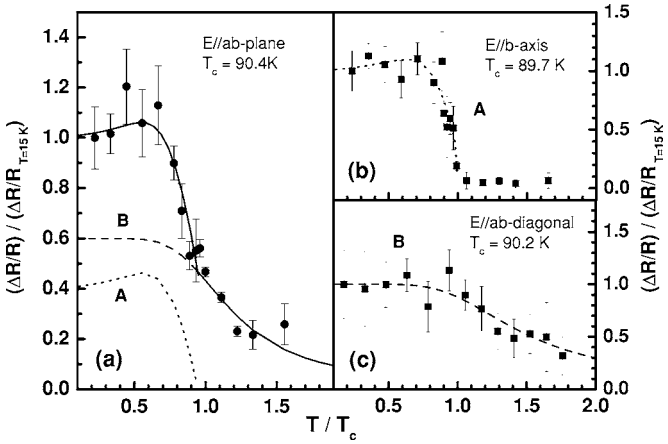

FIG. 2. The normalized $\Delta R/R$ as a function of the reduced temperature (a) in the *ab* plane of (001) YBCO films; (b) along the *b* axis of (100) YBCO films; and (c) along the *ab* diagonal of (110) YBCO films. The dotted and dashed lines are guides to the eye emphasizing the *A*- and *B*-type temperature dependences, respectively. The solid line in (a) shows the sum of the contribution from *A* and *B* temperature dependences.

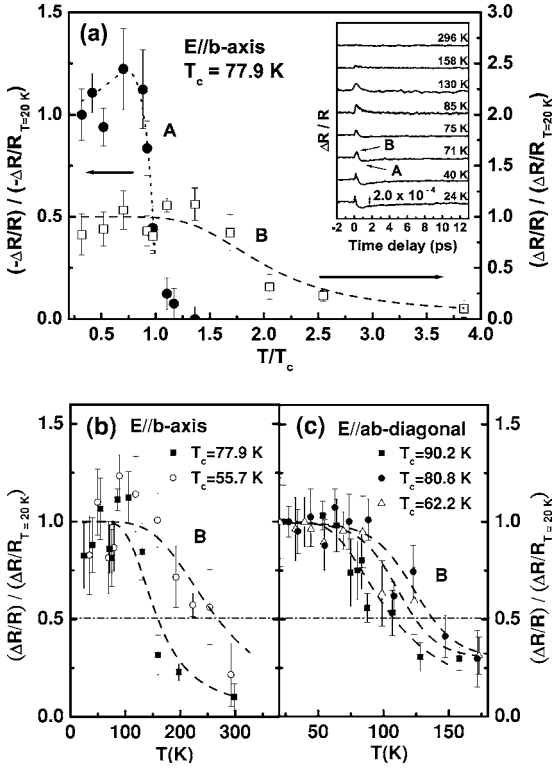

FIG. 3. (a) The normalized $\Delta R/R$ as a function of the reduced temperature along the b axis for T_c=77.9 K in a (100) YBCO film, which is the same one as in Fig. 1(b) and subsequently treated by the encapsulated bulk annealing method to manipulate the oxygen content (Ref. 23). Note: the solid and open symbols are, respectively, the negative and positive components in the inset which is the raw data of temperature-dependent $\Delta R/R$. (b) The normalized $\Delta R/R$ as a function of temperature along the b axis for various oxygen deficiencies were measured in a (100) YBCO film. (c) The normalized $\Delta R/R$ as a function of temperature along the ab diagonal for various oxygen deficiencies were measured in a (110) YBCO film. Dotted and dashed lines are guides to the eye emphasizing the A- and B-type temperature dependences, respectively.

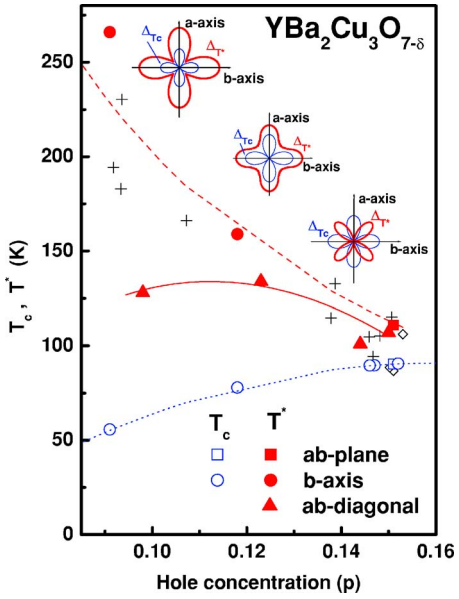

FIG. 4. (Color online) The critical temperature T_c and T^* as a function of hole concentration (p). The crosses and open diamonds are taken from the femtosecond time-resolved data reported by Demsar *et al.* (Ref. 8). The dashed line represents $T^* \propto 1/p$, where p is the hole concentration. The dotted line is drawn by the empirical relation $T_c(p)=T_{c,\max}[1\text{-}82.6(p\text{-}0.16)^2]$ with $T_{c,\max}$=91 K (Ref. 26). The solid line is a guide to the eye emphasizing the behavior of T^* along the ab diagonal. The points in near optimal doping were measured in several different samples, showing the generic nature of the observed behaviors. The insets illustrate the proposed scenario for the doping-dependent spatial symmetry of the Δ_{Tc} (thin-blue lines) and the Δ_{T^*} (thick-red lines).

as a function of hole doping along various orientations, the characteristic temperature (T^*) where $\Delta R/R$ drops to one half of its maximum value at low temperatures [the dashed-dotted line in Figs. 3(b) and 3(c)] is shown as a function of p in Fig. 4 together with T_c. Here, we should emphasize that the qualitative p dependence of T^* would remain the same, although different criteria for its determination (e.g., T^* is the temperature where the $\Delta R/R$ drops to one third of its low temperature value) would give a different absolute value of T^*. A closer look at the data displayed in Fig. 4, in fact, depicts the evolution of T_c and T^* as a function of p along various crystalline orientations in YBCO. Along the b axis, the systematic variation of $T^*$with p is similar to the one (crosses in Fig. 4) obtained in (001) YBCO films[8] and qualitatively follows the doping dependence of the pseudogap temperature T^* extracted by other experimental techniques. Besides, the superconductivity related to T_c was also clearly observed along the b axis and presented by the open circles in Fig. 4. On the other hand, along the ab diagonal, the component (A-type temperature dependence) related to T_c completely disappears and only the other component (B-type temperature dependence) T^* was observed at various hole concentrations (p). With decreasing p, T^* along the ab diagonal first increases and then decreases below p=0.12. Meanwhile, T^* along the b axis keeps increasing with decreasing p (dashed line in Fig. 4).

These results unambiguously indicate the spatial dichotomy of QP dynamics for the node (ab diagonal) and antinode (b axis), that are consistent with the observation in cuprate superconductors by ARPES.[4,5] In Ref. 4, the difference of the low energy excitations between nodal and antinodal QP, which is possibly associated with QPs scattering across the nearly parallel segments of the Fermi surface near antinodes, was clearly observed in underdoped $(La_{2-x}Sr_x)CuO_4$. Also, the dichotomy between the sharp nodal QP and broad antinodal states has been revealed in lightly doped $Ca_{2-x}Na_xCuO_2Cl_2$.[5] Moreover, by the non-spatial-resolved QP dynamics measurements, Gedik *et al.*[28] have claimed that the abrupt change in the sign of ΔR and the kinetics of QP decay in $Bi_2Sr_2Ca_{1-y}Dy_yCu_2O_{8+\delta}$ crystal is due to the dichotomy between coherent nodal QP excitations and incoherent antinodal excitations.

This dichotomy scenario is depicted from a perspective of gaps. The values of gaps (Δ_{Tc}, Δ_{T^*}) along the node and antinode can be simply estimated similar to the BCS result, $\Delta \propto k_B T_c$, with T_c and T^* in Fig. 4. For optimal-doped YBCO, Δ_{Tc} appears along the b axis while it is absent along the ab

diagonal. In contrast, Δ_{T^*} emerges along the *ab* diagonal while is absent along the *b* axis. The spatial symmetry of both gaps is illustrated schematically in the right inset of Fig. 4.[29] The $d_{x^2-y^2}$-symmetry for Δ_{Tc} has been demonstrated in an earlier femtosecond spectroscopy report.[9] Owing to the coexistence of Δ_{Tc} and Δ_{T^*} along the *b* axis for T_c=77.9 K, the nodes of Δ_{T^*} along the *b* axis disappear; meanwhile, the magnitude of Δ_{T^*} along the *ab* diagonal slightly increases with decreasing *p* as shown schematically in the middle inset of Fig. 4. Although the observed symmetry evolution of Δ_{T^*} seems unique, this picture is consistent with the symmetry evolution of the magnetic excitation in a recent inelastic neutron scattering experiment.[30,31] In Ref. 31, the high-energy magnetic excitation peaks, which is possibly associated with Δ_{T^*}, appear along (1,1) and $(1,\bar{1})$ directions in the two-dimensional (2D) reciprocal space. For the further underdoped case, the symmetry of Δ_{T^*} almost becomes $d_{x^2-y^2}$-symmetry as shown schematically in the left inset of Fig. 4. In this case, the symmetry ofΔ_{T^*} appear to shift from d_{xy} to $d_{x^2-y^2}$, though remains *d*-wave symmetry, with decreasing hole doping since Δ_{T^*} along the *ab* diagonal is shrinking while its value grows along the *b* axis. Under this approach, the dichotomy effect may be enhanced in the chain ordering phase, i.e., underdoped $YBa_2Cu_3O_{6.5}$ in the ortho II structure which has been studied by Segre *et al.*[32] and provides a different perspective for the decay rate of $\Delta R/R$ as the inelastic scattering rate of QP as well as the thermalization rate decreases with the development of the pseudogap.

The suppression of superconductivity in the underdoped regime seems to be due to the development of a competing order parameter Δ_{T^*} along the *b* axis which peaks along the *ab* diagonal at optimal doping. This further suggests that the intrinsic origins of the superconducting gap and the high-energy gap are different. Due to the ARPES evidence that a pseudogap state with a nodal-antinodal dichotomous character exists in the colossal magnetoresistive bilayer manganite $La_{1.2}Sr_{1.8}Mn_2O_7$ which is markedly different from a superconductor, Mannella *et al.*[33] cast doubt on the assumption that the pseudogap state in the copper oxides and the nodal-antinodal dichotomy are hallmarks of the superconductivity state. It means that the pseudogap state may be the universal characteristic in strongly correlated electron systems and strongly suggests that the pseudogap state may be irrelative to the superconducting state. Our paper thus provides one possible scenario of identifying the symmetry of the highly debated Δ_{T^*} and reveals how it evolves with hole-doping directly via the raw data of the time-resolved spectroscopy measurements. Certainly, there are some alternative routes open to approach this issue, such as the anisotropy of the probe transition matrix elements.[19] Dvorsek *et al.*[19] reported that the probe polarization dependence and the sign change of the transient signal below T_c is qualitatively described by the anisotropy of the probe transition matrix elements in Y124, and may not give the direct information regarding the anisotropy of the superconducting gap structure. Therefore, the validity of attributing the obtained experimental results to the symmetry change of high-energy gap Δ_{T^*} should be judged by further experiments and more developed theories.

IV. CONCLUSIONS

In summary, the spatial-temporal-resolved femtosecond spectroscopy unambiguously reveals the spatial dichotomy between nodal and antinodal QP relaxation dynamics. With the precise control of the oxygen content (i.e., the hole concentration) over one single film, we are able to track down the evolution of the respective spatial dichotomy with doping. From the possibly doping-dependent symmetry evolution of the two gaps, the important differences in the symmetry and origin between the high-energy gap (Δ_{T^*}) and superconducting gap (Δ_{Tc}) in YBCO are recognized.

ACKNOWLEDGMENTS

This work was supported by the National Science Council of Taiwan, Republic of China under Grants Nos. NSC94-2112-M009-005, NSC95-2112-M-009-037-MY3, NSC95-2112-M-009-011-MY3, and by the Grant MOE ATU Program at NCTU.

[1] P. W. Anderson, P. A. Lee, M. Randeria, T. M. Rice, N. Trivedi, and F. C. Zhang, J. Phys.: Condens. Matter **16**, R755 (2004).
[2] C. M. Varma, Phys. Rev. B **55**, 14554 (1997); C. M. Varma, cond-mat/0312385 (unpublished).
[3] T. Yoshida, X. J. Zhou, T. Sasagawa, W. L. Yang, P. V. Bogdanov, A. Lanzara, Z. Hussain, T. Mizokawa, A. Fujimori, H. Eisaki, Z.-X. Shen, T. Kakeshita, and S. Uchida, Phys. Rev. Lett. **91**, 027001 (2003).
[4] X. J. Zhou, T. Yoshida, D.-H. Lee, W. L. Yang, V. Brouet, F. Zhou, W. X. Ti, J. W. Xiong, Z. X. Zhao, T. Sasagawa, T. Kakeshita, H. Eisaki, S. Uchida, A. Fujimori, Z. Hussain, and Z.-X. Shen, Phys. Rev. Lett. **92**, 187001 (2004).
[5] K. M. Shen, F. Ronning, D. H. Lu, F. Baumberger, N. J. C. Ingle, W. S. Lee, W. Meevasana, Y. Kohsaka, M. Azuma, M. Takano, H. Takagi, and Z.-X. Shen, Science **307**, 901 (2005).
[6] C. W. Luo, K. Reimann, M. Woerner, T. Elsaesser, R. Hey, and K. H. Ploog, Phys. Rev. Lett. **92**, 047402 (2004).
[7] R. A. Kaindl, M. Woerner, T. Elsaesser, D. C. Smith, J. F. Ryan, G. A. Farnan, M. P. McCurry, and D. G. Walmsley, Science **287**, 470 (2000).
[8] J. Demsar, B. Podobnik, V. V. Kabanov, T. Wolf, and D. Mihailovic, Phys. Rev. Lett. **82**, 4918 (1999).
[9] C. W. Luo, M. H. Chen, S. P. Chen, K. H. Wu, J. Y. Juang, J.-Y. Lin, T. M. Uen, and Y. S. Gou, Phys. Rev. B **68**, 220508(R) (2003).
[10] C. W. Luo, P. T. Shih, Y.-J. Chen, M. H. Chen, K. H. Wu, J. Y. Juang, J.-Y. Lin, T. M. Uen, and Y. S. Gou, Phys. Rev. B **72**, 092506 (2005).
[11] S. G. Han, Z. V. Vardeny, K. S. Wong, O. G. Symko, and G. Koren, Phys. Rev. Lett. **65**, 2708 (1990).
[12] J. M. Chwalek, C. Uher, J. F. Whitaker, G. A. Mourou, J. Agostinelli, and M. Lelental, Appl. Phys. Lett. **57**, 1696 (1990).

[13] G. L. Eesley, J. Heremans, M. S. Meyer, G. L. Doll, and S. H. Liou, Phys. Rev. Lett. **65**, 3445 (1990).
[14] D. H. Reitze, A. M. Weiner, A. Inam, and S. Etemad, Phys. Rev. B **46**, R14309 (1992).
[15] T. Gong, L. X. Zheng, W. Xiong, W. Kula, Y. Kostoulas, Roman Sobolewski, and P. M. Fauchet, Phys. Rev. B **47**, 14495 (1993).
[16] Y. Liu, J. F. Whitaker, C. Uher, J.-L. Peng, Z. Y. Li, and R. L. Greene, Appl. Phys. Lett. **63**, 979 (1993).
[17] V. V. Kabanov, J. Demsar, B. Podobnik, and D. Mihailovic, Phys. Rev. B **59**, 1497 (1999).
[18] J. Demsar, B. Podobnik, J. E. Evetts, G. A. Wagner, and D. Mihailovic, Europhys. Lett. **45**(3), 381 (1999).
[19] D. Dvorsek, V. V. Kabanov, J. Demsar, S. M. Kazakov, J. Karpinski, and D. Mihailovic, Phys. Rev. B **66**, 020510(R) (2002).
[20] C. W. Luo, M. H. Chen, S. J. Liu, K. H. Wu, J. Y. Juang, T. M. Uen, J.-Y. Lin, J.-M. Chen, and Y. S. Gou, J. Appl. Phys. **94**, 3648 (2003).
[21] S. J. Liu, J. Y. Juang, K. H. Wu, T. M. Uen, Y. S. Gou, J. M. Chen, and J.-Y. Lin, J. Appl. Phys. **93**, 2834 (2003).
[22] C. W. Luo, M. H. Chen, C. C. Chiu, K. H. Wu, J. Y. Juang, T. M. Uen, J.-Y. Lin, and Y. S. Gou, J. Low Temp. Phys. **131**, 545 (2003).
[23] K. H. Wu, M. C. Hsieh, S. P. Chen, S. C. Chao, J. Y. Juang, T. M. Uen, Y. S. Gou, T. Y. Tseng, C. M. Fu, J. M. Chen, and R. G. Liu, Jpn. J. Appl. Phys., Part 1 **37**, 4346 (1998).This method is capable of controlling the oxygen content of the YBCO films precisely and reversibly. It is worth emphasizing that, by using this method, all the measurements with various oxygen contents can be performed on *one single YBCO film* to avoid any possible complication from individual film structures and to make sure that any properties changes should be due to the variation in the oxygen content.
[24] C. J. Stevens, D. Smith, C. Chen, J. F. Ryan, B. Podobnik, D. Mihailovic, G. A. Wagner, and J. E. Evetts, Phys. Rev. Lett. **78**, 2212 (1997).
[25] The hole concentration of each sample was estimated by $T_c = T_{c,\max}\,[1\text{-}82.6(p\text{-}0.16)^2]$ with $T_{c,\max}=91$ K Ref. 26.
[26] J. L. Tallon, C. Bernhard, H. Shaked, R. L. Hitterman, and J. D. Jorgensen, Phys. Rev. B **51**, R12911 (1995).
[27] The change of $\Delta R/R$ sign is due to the shifting of Fermi surface as a function of the hole concentration.
[28] N. Gedik, M. Langner, J. Orenstein, S. Ono, Y. Abe, and Y. Ando, Phys. Rev. Lett. **95**, 117005 (2005).
[29] However, ARPES Ref. 30 shows that the symmetry of pseudogap remains as a $d_{x^2-y^2}$ regardless of the hole concentration. The difference between our results and ARPES may simply arise from the fact that ARPES gives rather direct information about the QP spectrum while the pump-probe spectroscopy provides relatively indirect spectrum convolved with itself as well as relevant inelastic scattering processes such as phonons, magnons, etc.
[30] A. Damascelli, Z. Hussain, and Z. X. Shen, Rev. Mod. Phys. **75**, 473 (2003).
[31] S. M. Hayden, H. A. Mook, Pengcheng Dai, T. G. Perring, and F. Doğan, Nature (London) **429**, 531 (2004).
[32] G. P. Segre, N. Gedik, J. Orenstein, D. A. Bonn, R. Liang, and W. N. Hardy, Phys. Rev. Lett. **88**, 137001 (2002).
[33] N. Mannella, W. L. Yang, X. J. Zhou, H. Zheng, J. F. Mitchell, J. Zaanen, T. P. Devereaux, N. Nagaosa, Z. Hussain, and Z.-X. Shen, Nature (London) **438**, 474 (2005).